CE-ICP-MS to probe Aβ1-42/copper (II) interactions, a complementary tool to study amyloid aggregation in Alzheimer's disease

Coraline Duroux, Agnès Hagège

CE-ICP-MS to probe $A\beta_{1-42}$ / copper (II) interactions, a complementary tool to study amyloid aggregation in Alzheimer's Disease

C. Duroux, A. Hagège*

Université de Lyon, CNRS, Université Claude Bernard Lyon 1, Institut des Sciences Analytiques, UMR 5280, 69100 Villeurbanne, France, e-mail: agnes.hagege@isa-lyon.fr

Running head title: CE-ICP-MS to probe $A\beta_{1-42}$ / copper (II) interactions

Abstract: Copper (II) ions appear to be involved in the Alzheimer's disease (AD) and seem to influence the aggregation of the amyloid-β_{1-42} ($A\beta_{1-42}$) peptide. However, data are not conclusive and still not subject to consensus, copper (II) being suspected to either promote or inhibit aggregation. To address this question, CE-ICP-MS hyphenation was proposed as a complementary tool to follow the distribution of copper in the different oligomeric forms, at different sub-stoichiometries and different incubation times. Results clearly indicated the formation of several negatively charged copper complexes and showed the enhancement of the aggregation rate with copper concentration. Moreover, the variations of copper (II) speciation suggest different aggregation pathway, even for sub-stoichiometric ratios.

Keywords: amyloid-β ; oligomerization ; copper speciation ; CE-ICP-MS hyphenation ; labile complexes ; voltage induced dissociation

Introduction

Alzheimer's disease (AD) is one of the most common forms of dementia in the world, characterized by progressive cognitive and memory impairments. However, the treatments are further hampered by the lack of understanding of the highly complex mechanisms at the origin of AD. While it now seems accepted that amyloid-β peptides ($A\beta$), mainly $A\beta_{1-40}$ and $A\beta_{1-42}$, play a central role, their mode of action is not yet understood. Although the aggregation of the peptide appears to be a crucial step, many questions remain unsolved about the toxicity of oligomerized species of $A\beta$. Toxicity, initially attributed to the presence of senile plaques,[1] seems to be now caused by small soluble oligomers of these peptides.[2]

In addition, the involvement of metals such as copper (Cu), zinc (Zn), and iron (Fe) seem to be accepted and is supported by various observations.

As far as Cu is concerned, micro-PIXE analyses performed by Lovell *et al.* indicated a significant increase in Cu in amyloid plaques rims.[3] Cu and Zn observed in brain by SXRF microprobe were also reported to be localized in high β-sheet content regions.[4] However, even if a co-localization of Cu with these amyloid plaques was ascertained[3,4], some authors reported a non-significant increase of Cu amounts associated with Aβ plaques in brain regions of Alzheimer patients, compared to the basal Cu levels.[5] Conversely, ICP measurements of 7 brain regions from 9 cases with AD revealed a copper deficiency in all AD brain regions.[6]

Apparently contradictory findings were also reviewed about the influence of Cu(II) on aggregation.[7] Both promoting[8,9] and inhibiting effects[10-12] of copper binding on aggregation were reported. $A\beta_{1-42}$ aggregation is an intricate problem since many parameters, such as pH, temperature, and concentrations affect this phenomenon. However, Cu(II) appears to be one of the driving forces in the conformational changes of the $A\beta_{1-42}$ in different oligomerized forms with various structures and sizes, such as pre-fibrillar oligomers, fibrillar oligomers and annular protofibrils.[13] Pedersen *et al.* proposed the existence of copper-dependent aggregation pathways.[12] It was suggested that the presence of Cu (II) in high concentration leads to the formation of amorphous deposits prone to precipitation. However, under stoichiometric ratios, Cu(II) might accelerate β-sheet formation, promoting the appearance of thioflavin-T reactive fibrils species.[14] Little data have been published on the aggregation kinetics of $A\beta_{1-42}$ upon addition of sub-equimolar amounts of Cu(II). In these conditions, Cu was found to lead to the formation of oligomers and even to the disassembly of fibres.[15]

Although many studies have been devoted to this problem, most of them were focused on amyloid-β peptide's conformation, structure and properties variations upon copper addition. Developments of speciation approaches allowing the study of the association of metals with the oligomers of these Aβ are scarce. No changes in Cu(II) coordination environment were detected in EPR when bound to $A\beta_{1-40}$ in various oligomeric states[8] which seems to preclude its use in speciation analysis. The coupling of ion mobility with mass spectrometry was used to demonstrate the stabilization of metal-induced compact forms of $A\beta_{1-40}$ oligomers, from trimers to pentamers, in the presence of metal ions such as Cu^{2+} and Zn^{2+}. Although recorded mass spectra correspond to metal-free oligomers, the slow interconversion between compact species and extended species allowed to retain the metal-bound drift time profile in their metal-free form.[16]

The aim of the presented research was to propose an analytical approach to assess the distribution of Cu (II) among the different $A\beta_{1-42}$-species. Directly assessing metal-Aβ complexes requires an analytical method allowing a minimal disruption of the complexes. Capillary zone electrophoresis coupled to ICP-MS was successfully used for the analysis of several metal-protein complexes.[17-20] However, owing to the small size of the peptides and oligomers and the lability of copper complexes, analysis of Cu(II) complexes of $A\beta_{1-42}$ remains a difficult challenge. Capillary zone electrophoresis was demonstrated to be able to separate Aβ monomer and oligomers,[21-25] but to our knowledge, only one study looked at the fate of both amyloid-β peptides and Cu. However, only total Cu concentrations were measured by ICP-MS after centrifugation and no speciation data were provided.[12]
Here the use of coupling of capillary electrophoresis to ICP-MS has been proposed to study the influence of Cu(II) on $A\beta_{1-42}$ aggregation and evaluate the Cu content of oligomers during the aggregation process.

Materials and methods

Products
$A\beta_{1-42}$ and $A\beta_{1-16}$ (purity ≥ 95%) were purchased as lyophilized powder from GeneCust (Boynes, France) and used without further purification. Tris (Trizma® base), sodium chloride, hydrochloric acid 37%, tributyl phosphate (TBP) 99% and EDTA were obtained from Sigma-Aldrich. Nitric acid 1% was obtained by dilution in water of HNO_3 65% (Suprapur® quality) purchased from Merck. Stock solution of Cu(II) at 500 µM in 10 mM Tris, 15 mM NaCl at pH 7.4 was obtained via dissolution of $CuCl_2.2H_2O$ purchased from Merck. Acetone (0.1% in water) and tributylphosphate (TBP 0.03% in DMSO 2%) purchased from Sigma-Aldrich were used as neutral species markers for CE-UV and CE-ICP-MS respectively.
Since Cu is one of the most difficult element to analyze at trace levels, extreme caution was taken to avoid external contamination (see SI). All products were analysed regarding to their Cu content by ICP-MS and compared with a reference value obtained for copper at 5 ppb. Products with contamination greater than the one measured for HNO_3 1% were discarded (a few tens of ppt). Before use, labware was cleaned three times with nitric acid 1%. These precautions drastically improve the background level which can however not fall below 600 cps.
Fused-silica capillaries were purchased from Polymicro Technologies (Phoenix, AZ). A hydroxypropyl cellulose (HPC) thermal coating of the capillaries (I.D of 75 µm, O.D of 375 µm, 64 cm total length)[26] was performed using a HPC solution, 0.05 g/ mL in water in order to limit the interactions between the silanols of the capillary surface and the copper ions.

Peptide samples preparation
Stock solutions of $A\beta_{1-42}$ at 250 µM were prepared by direct dissolution of lyophilized $A\beta_{1-42}$ in 0.1% (m/v) ammonium hydroxide aqueous solution. Stock solutions of $A\beta_{1-16}$ at 500 µM were prepared by direct dissolution of lyophilized $A\beta_{1-16}$ in 10 mM Tris, 15 mM NaCl at pH 7.4. Aβ peptides concentration was determined by UV measurements (Thermo Scientific™ NanoDrop™ UV-Vis Spectrophotometer) at 280 nm (ε = 1490 $M^{-1}cm^{-1}$ for both peptides, from UniProtKB/Swiss-Prot Database). These solutions were checked to be stable over one week, when stored at 4°C.
Before each study, Aβ peptides were diluted in 10 mM Tris, 15 mM NaCl at pH 7.4 and varying volumes of the stock solution of Cu(II) were added in order to obtain a final peptide concentration of 100 µM in 8 mM Tris, 10 mM NaCl at pH 7.4, in the presence of different concentrations of Cu(II).

Taylor dispersion analysis (TDA) for $A\beta_{1-42}$ size measurements
TDA experiments were conducted using a Beckman P/ACE MDQ instrument in HPC capillaries. After injection (0.5 psi, 5 s, i.e. 23.5 nL), samples were mobilized with an applied pressure of 0.7 psi. The mobilization medium used was a Tris 10 mM, NaCl 15 mM buffer at pH 7.4 and detection was performed by UV at 200 nm with a data acquisition rate of 16 Hz (detection length: 54 cm). Between runs, the capillary was flushed at 10 psi for 5 min with the mobilization medium.
The taylorgrams obtained by TDA can be assimilated to the sum of several Gaussians signals:

$$S(t) = \sum_{i=1}^{n} \frac{A_i}{\sigma_i \sqrt{2\pi}} \exp\left(-\frac{(t-t_0)^2}{2\sigma_i^2}\right) \quad (1)$$

where t_0 is the peak residence time and A_i and σ_i are the area under the curve and temporal variance associated to the different species I, respectively.

Under these experimental conditions, the molecular diffusion coefficient D is given by equation 2 and can be related to the hydrodynamic radius of the species.

$$D = \frac{r_c^2 t_0}{24\sigma^2} = \frac{k_B T}{6\pi\eta R_h} \quad (2)$$

where r_c is the capillary radius, k_B is the Boltzmann constant, T is the temperature, η is the viscosity, and R_h is the hydrodynamic radius of the solute. For a Tris 10 mM, NaCl 15 mM buffer, the viscosity was previously measured and found to be 0.908.

Deconvolution and integration of the peak was performed using the Origin 8.5 software, assuming ε_{200nm} to be equal for all $A\beta_{1-42}$ species.

Aggregation monitoring using CE-UV

CE experiments were carried out on a Beckman P/ACE MDQ instrument, using HPC capillaries. The background electrolyte (BGE) was 10 mM Tris, 15 mM NaCl at pH 7.4. Prior to the first use, the capillary was flushed with water and BGE for 5 min under 10 psi. Samples were introduced into the capillary by hydrodynamic injection under 0.5 psi for 5 sec (i.e. 23.5 nl). Separations were performed at 25°C at -20 kV with an assisted pressure of 0.1 psi. Since amyloid-β compounds have relatively low electrophoretic mobility, this additional pressure was necessary to compensate the absence of electroosmotic mobility in a neutral capillary such as HPC. The assisted pressure leads to a reduced residence time in the capillary but also to the formation of a Poiseuille flow affecting the peak width, and consequently the resolution. Detection was performed by UV at 200 nm at 54 cm from the inlet with an acquisition rate of 16 Hz. Data were collected using the 32 Karat Software. Between runs, the capillary was rinsed with the BGE for 5 min under 10 psi.

Calculation of $A\beta_{1-42}$ species content was performed using the classical correction of peak areas in CE (measured area divided by migration time), assuming ε_{200nm} to be equal for all $A\beta_{1-42}$ species.

Determination of copper distribution using CE-ICP-MS

For CE-ICP-MS hyphenation, the ICP-MS instrument used as detector was an Agilent 7700 equipped with a MicroMist nebulizer. The spectrometer was controlled by the MassHunter software. Hyphenation was achieved *via* a home-made sheath-flow interface. The capillary goes first through a microcross piece toward the tip of the nebulizer. The electrical connection was achieved by the ground electrode positioned through the third inlet of the microcross. The sheath liquid (Tris 5 mM, pH 7.4 containing 10 µM EDTA to warrant the absence of copper sorption on ICP-MS glass parts) was introduced by self-aspiration to the fourth inlet of the interface. The sheath liquid solution height was adjusted by means of an elevator to both eliminate the suction effect due to the nebulizer and avoid any flow reversal into the capillary following the procedure described elsewhere.[27] The optimal flow was estimated to be around 450 µL.min^{-1} by measuring the sheath flow consumption over a 30 min period. This interface was checked not to introduce significant external dispersion (see supplementary information).

Samples were introduced into the HPC capillary by hydrodynamic injection under 1 psi for 10 sec (i.e. around 90 nL). Electrophoretic separations were performed at 25°C at -7 kV assisted by a pressure of 0.3 psi. Cu was detected by ICP-MS at m/z = 65 (dwell time 1 s) at the end of the capillary (64 cm). ICP operating conditions were: carrier gas flow rate: 1 L.min^{-1}, makeup gas flow rate: 0.1 L.min^{-1}, plasma gas flow rate: 15 L.min^{-1}, auxiliary gas flow rate: 0.9 L.min^{-1}, radiofrequency power 1550 W for the plasma, other parameters were tuned in order to maximize the signal. Between runs, the capillary was rinsed with nitric acid 1% for 10 min under 5 psi and with the BGE for 5 min under 5 psi.

Integration of the Cu(II) containing peaks was performed using Origin 8.5 by minimizing an exponentially modified Gauss function, as proposed by Sauge-Merle *et al.*[28], when using low resolution conditions (i.e. 5kV + 0.5 psi in their case).

Results and discussion

Identification of Aβ$_{1-42}$ species

In order to follow Aβ$_{1-42}$ aggregation, attempts to identify the different of Aβ$_{1-42}$ species within electrophoregrams were performed. For that purpose, two different solutions containing 100 µM Aβ$_{1-42}$ were prepared: one solution prepared in self-aggregating conditions, i.e. incubated for 48h at room temperature in the electrolyte at pH 7.4, another one in conditions limiting aggregation, i.e. freshly prepared in NH_4OH 0.1%.

Analyses of both samples were realized in capillary electrophoresis at -20 kV + 0.1 psi in a HPC-modified capillary using Tris 10 mM, NaCl 15 mM, pH 7.4 as background electrolyte. The resulting electropherograms are presented in Figure 1.

The electrophoretic mobilities (μ_{ep}) were determined by subtracting the Poiseuille flow contribution, using acetone as a neutral marker (NM) and thanks to the equation 3**:**

$$\mu_{ep} = \frac{L_d L_t}{V} * (\frac{1}{t_m} - \frac{1}{t_{NM}}) \quad (3)$$

where L_d is the length of detection, L_t is the total length of the capillary, V is the applied voltage, t_m is the migration time of the analyte peak and t_{NM} is the migration time of the neutral marker peak.

Apart from the first peak attributed to the presence of NH_4OH by direct injection of a 0.05% NH_4OH, both mobilograms exhibit two main peaks (1 and 2), with electrophoretic mobilities of - 2x10^{-8} m²V^{-1}s^{-1} and - 1x10^{-8} m²V^{-1}s^{-1} respectively (Fig.1a).

Peak areas were measured for both peaks and the respective percentages of both species were calculated from the corrected peak areas (peak area/migration time). Results are presented in Table 1.

In parallel, TDA experiments were performed using the same capillary and the same electrolyte as mobilization buffer. The taylorgrams were shown to be successfully fitted by a trimodal fitting, indicating the presence of three different species in the two samples (Fig.1b). The sharpest deconvoluted peak was attributed to NH_4OH since the diffusion coefficient experimentally determined ((1.3 ± 0.3) 10^{-9}m^2.s^{-1}) was similar to the one tabulated for NH_4OH at 20°C (1.5.10^{-9} m^2.s^{-1}). Both hydrodynamic radii and percentages of the other two species were calculated and compared in Table 1.

Based on these results, the presence of two different populations containing Aβ$_{1-42}$ was assumed: one fast migrating population (μ_{ep} ~ -2 x10^{-8}m^2.s^{-1}.V^{-1}) with a large hydrodynamic radius, attributed to large oligomers, and one population migrating slower (μ_{ep} ~ -1 x10^{-8}m^2.s^{-1}.V^{-1}) with a smaller hydrodynamic radius, attributed to monomers and small oligomers.

This assumption is reinforced by the data obtained by Deleanu *et al.*[29], who proposed possible conformations of Aβ$_{1-42}$ in relation with their size determined by TDA. They found a population of monomers and small oligomers, with a mean hydrodynamic radius around 1.9 nm, and a population of larger oligomers, with a mean radius around 5.1 nm. Moreover, several groups reported the μ_{ep} of Aβ$_{1-42}$ oligomers and monomer at pH 7.4[21-23] and showed that oligomers present a mobility which is twice the one of monomers.

Separation conditions preserving copper complexes

The separation of Aβ$_{1-42}$ species is well-described in literature[21-25] and was performed at -20kV + 0.1 psi on a neutral HPC capillary without further improvement.The repeatability of mobilities was determined by performing three CE separations of a partially aggregated peptide Aβ$_{1-42}$. Results indicated a relative standard deviation not exceeding 5% for mobilities allowing the use of this method for the monitoring of the different species over time.

However, the separation of the Cu(II)-complexes monitored by CE-ICP-MS in such analytical conditions is severely marred by the observation of strongly tailing peaks, due to the partial dissociation of the complexes during separation.

Optimization of separation conditions was carried out, to face the disequilibrium effects linked to the analysis of copper complexes. Indeed, kinetically fast metals like Cu(II) may form labile complexes, which are likely to dissociate during the separation.[30]

As this dissociation may be increased by the application of voltage, experiments were carried out with different voltages. For that purpose, $A\beta_{1-16}$ was chosen as reference compound since it contains the same complexation site than $A\beta_{1-42}$ and is not subject to aggregation.
Figure 2 presents the results obtained for the CE-ICP-MS analysis of solutions containing 100 µM $A\beta_{1-16}$ and either 10 µM or 50 µM Cu(II). The electropherograms show distorted peaks, composed of a nearly Gaussian part corresponding to the $A\beta_{1-16}$-Cu(II) complex, and a tailing part, corresponding to the copper dissociated from this complex (Fig. 2a). For the different voltages, Gaussian peak, tailing part and Cu(II) peak released by HNO_3 rinses areas were calculated (Fig. 2b).
These results show that an increase of voltage leads to an increase of the tailing part of the peak (Fig. 2c and 2d). Moreover, the washing step using HNO_3 1% reveals a small but increasing amount of Cu adsorbed on the HPC capillary. Applying a high voltage such as -20kV leads to the dissociation of 2/3 of Cu(II) initially complexed, for both Cu(II) concentrations. By decreasing the voltage to -7 kV, more than 80% of the complex remains intact. However, these conditions dramatically affect the resolution and any additional decrease of the voltage would prohibit the separation of the $A\beta_{1-42}$ species.
As a consequence, -20kV + 0.1 psi was maintained in association with the UV detection to separate $A\beta_{1-42}$ species with a good resolution and -7kV + 0.3 psi was applied when using the ICP-MS detection to perform the separation of Cu(II) complexes while limiting the dissociation.
As $A\beta_{1-42}$ undergoes self-aggregation over the time, repetability on peak areas, linearity and limit of quantification cannot be evaluated using such a sample. Consequently, $A\beta_{1-16}$ was used instead of $A\beta_{1-42}$, to overcome variations due to speciation changes during aggregation (see supplementary information).
Although all the analytical figures of merit (Table 3) cannot be directly transposed to the analysis of $A\beta_{1-42}$, they may be representative of the method.

Does copper accelerate the aggregation of the $A\beta_{1-42}$ peptide?

This CE-UV method was used in order to study the influence of the presence of Cu on the aggregation kinetics of the $A\beta_{1-42}$ peptide. For that purpose, kinetic monitoring was carried out, for several $A\beta_{1-42}$: copper initial ratios (1: 0, 1: 0.1 and 1: 0.5). Incubations of 100 µM of $A\beta_{1-42}$ in the presence of different Cu(II) concentrations (10 and 50 µM) were performed at room temperature. The solutions were analysed at different incubation times and compared with the results obtained for a 100 µM of $A\beta_{1-42}$ solution in the absence of Cu. All the results are averages from two different kinetic experiments for each $A\beta_{1-42}$: Cu(II) ratio and are presented in Fig. 3.

All the electropherograms (Fig. 3a) exhibit two main peaks, with electrophoretic mobilities - $2x10^{-8}$ $m^2V^{-1}s^{-1}$ and - $1x10^{-8}$ $m^2V^{-1}s^{-1}$. Previous affinity capillary electrophoresis studies performed in the presence of Cu(II) in the electrolyte have shown that Aβ and Aβ-Cu complexes exhibit only slight differences in electrophoretic mobilities (see supplementary information). Peaks 1 and 2 were therefore attributed to large oligomers and small oligomers/monomer respectively. Peak 1, observed in many studies in the absence of copper, was not observed by Pedersen *et al.* in the presence of this metal with $A\beta_{1-40}$.[12] Indeed, it was postulated that $A\beta_{1-40}$ displays a different aggregation pathway, which does not lead to the formation of transient soluble oligomers.[29]

Fig. 3b shows the percentage of $A\beta_{1-42}$ involved in large oligomers in the soluble fraction. This was determined by calculating the ratio of large oligomeric forms area to the total area in UV, using corrected areas to correct the influence of the different velocities on the signal measurement and assuming $\varepsilon_{A\beta \text{ in monomer}}$ to be equal to $\varepsilon_{A\beta \text{ in oligomer species}}$ at 200 nm. The distribution of $A\beta_{1-42}$ between the different soluble species was calculated as follows:

$$\%A\beta_{1\text{-}42,\ \text{species I}} = \frac{\text{Corrected peak area}_{\text{species i}}}{\sum_{j=1}^{n} \text{Corrected peak area}_{\text{species j}}} \quad (4)$$

Such calculations allow to compensate for the absence of calibration curve (impossible to obtain for $A\beta_{1-42}$).
Surprisingly, no immediate precipitation of $A\beta_{1-42}$ was observed whatever the copper concentration in the sample. This was verified by measuring both UV absorbance at 280 nm and copper concentration by ICP-MS at the beginning and the end of the experiment. Moreover, Σ corrected peak area was found to be constant over the time with a relative standard deviation of 10%. In our case, percentages can be directly converted into $A\beta_{1-42}$ concentrations.

Data obtained at t=0 for the copper-free sample illustrate the strong ability of $A\beta_{1-42}$ peptide to instantaneously self-aggregate upon dissolution in the buffer despite the presence of NH_4OH. This could be due to the high concentration of $A\beta_{1-42}$ (100 µM) used in this study, similar to concentrations usually used by others in *in vitro* kinetics studies. $A\beta_{1-42}$ involved in large oligomerized forms was found to be about 20%. By comparing the initial repartition for each Cu(II): $A\beta_{1-42}$ ratio, it could be noticed that the initial percentage of oligomerization increases in the presence of Cu(II) in the sample, to reach up to 35% for both initial ratios. This instantaneous aggregation observed in the presence of Cu(II) was already observed in studies on $A\beta_{1-40}$.[9,12]
The examination of the oligomerization kinetics curves (Fig. 3b) shows a similar profile with a propensity of the peptide to aggregate either with or without Cu(II). Whatever the Cu(II) concentration is, the percentage of peptide involved in oligomeric forms increases almost linearly with the incubation time to reach a plateau.
Therefore, the slope of the linear part reflects the apparent oligomerization velocity (in $\%.h^{-1}$). Results are summarized in Table 2. The apparent velocities either in the absence of copper or for 10 µM Cu(II) were similar, which does not reflect any significant influence of Cu for such a sub-stoichiometric ratio. However, in the presence of 50 µM Cu (II) in the sample, velocity was found ca. 10 times higher, indicating an increase in the kinetic of aggregation. The percentage at the plateau does not seem to depend on Cu(II) concentration and discrepancies observed with and without Cu seem to be due to the differences observed à t=0.

How is copper distributed among the different oligomeric forms?

Monitoring of the distribution of Cu among the different forms of the peptide was performed by CE-ICP-MS analyses of 100 µM $A\beta_{1-42}$ samples containing either 10 or 50 µM Cu(II). Experiments were performed in duplicates and results are presented in Fig. 4. For both samples (Fig. 4a and b), electropherograms show the presence of two negative copper complexes (peaks 1 and 2). The negative mobilities, calculated using TBP as a neutral marker (m/z = 31), are in agreement with the formation of negatively charged Aβ-Cu complexes. As a consequence of the combination of the application of low voltage and high pressure, the resolution was strongly affected. This peak overlapping hinders any accurate quantitative measurements but the separation remained sufficient to be able to distinguish both monomeric and oligomeric states of $A\beta_{1-42}$. Moreover, a significant peak broadening was observed for the so called-monomeric species, compared to the results obtained in UV (Fig. 3a), and might suggest the co-migration of both the monomer and the smallest oligomers, already observed in UV. In the presence of 50 µM of Cu(II) (Fig. 4b), an additional unknown peak was revealed, which might result from the presence of ammonium hydroxide in the solution, since a copper species with similar mobility was also observed in blank samples.

Calculation of copper percentages were performed as previously for the different peaks in the soluble fraction:

$$\%Cu_{,\ \text{species I}} = \frac{\text{Corrected peak area}_{\text{species i}}}{\sum_{j=1}^{n} \text{Corrected peak area}_{\text{species j}}} \qquad (5)$$

The absence of copper precipitation was checked by copper ICP-MS analyses at the beginning and at the end of each experiment.
Figure 4 shows a decrease of the "monomer and small oligomers" fraction for both stoichiometries as the aggregation progresses (Fig. 4c and 4d). In the 1: 0.1 Aβ: Cu sample, an increase over time of the percentage of Cu present in the larger oligomers fraction was observed, until nearly all the soluble copper was incorporated in this fraction (Fig. 4c). This increase is closely correlated to the increase of the $A\beta_{1-42}$ peptide involved in the larger oligomers forms (Fig. 3b). Such a trend might indicate a similar complexation of Cu in the different forms. Mold *et al.* assumed that it could reveal a kinetically favoured aggregation, to the detriment of complexation. As a result, this could explain the similarity of the conversion of monomer into larger oligomers in the absence and in the presence of 10 µM Cu.[31]
Increasing Cu(II) concentration to 50 µM led to a quite different behaviour. Cu involved in the larger oligomers fraction slightly increased, until a plateau representing 40-45% of the soluble copper (Fig. 4d). Comparison of this distribution with the one of $A\beta_{1-42}$ peptide in the soluble forms (Fig. 3b) suggests clearly that Cu is mainly present in the "monomer and small oligomers" fraction. Based on the researches so far, the aggregation process could be enhanced via the formation of an intermolecular copper complex.

Conclusion

CE-ICP-MS was used to monitor for the first time the distribution of Cu between soluble species of $A\beta_{1-42}$ and confirmed that Cu exhibits an affinity for both monomeric and oligomeric $A\beta_{1-42}$ species and lead to the formation of anionic species. The investigation of $A\beta_{1-42}$ oligomerization over time showed that Cu influences the rate of oligomerization and tends to distribute in both small and large oligomers. A clear difference in copper distribution was observed depending on the Cu(II) concentration used, which seems to be in agreement with the formation of intramolecular at low Cu(II) concentrations and intermolecular complexes for higher concentrations. Although the $A\beta_{1-42}$ concentrations used may not be representative of *in vivo* conditions and could favour self-aggregation, we showed that this method can provide valuable information in Aβ / copper complexation studies.

Moreover, such a study was impaired by the poor resolution of the separation, resulting from mild separation conditions optimized to avoid complexes dissociation. Since, a total separation of the species was not possible, an accurate quantitation of copper in the different species is precluded. Non-separative methods, such as Taylor dispersion analysis, allowing the discrimination of species according to their diffusion coefficient, could also be envisaged. The ability of TDA to be coupled with ICP-MS should provide useful information concerning the size of the copper species formed during the *in vitro* aggregation process. It is also of importance to be able to separate monomer from small oligomers and further investigations are still ongoing to achieve this goal.

Acknowledgements

This work was supported by the Doctoral School of Chemistry, University of Lyon, France (grant to CD). The authors have declared no conflict of interest.

References

1 J. A. Hardy and G. A. Higgins, Alzheimer's Disease: The Amyloid Cascade Hypothesis, Science, 1992, 256, 184–185.

2 P. Cizas, R. Budvytyte, R. Morkuniene, R. Moldovan, M. Broccio, M. Lösche, G. Niaura, G. Valincius and V. Borutaite, Size-dependent neurotoxicity of β-amyloid oligomers, Arch. Biochem. Biophys., 2010, 496, 84–92.

3 M. A. Lovell, J. D. Robertson, W. J. Teesdale, J. L. Campbell and W. R. Markesbery, Copper, iron and zinc in Alzheimer's disease senile plaques, J. Neurol. Sci., 1998, 158, 47–52.

4 L. M. Miller, Q. Wang, T. P. Telivala, R. J. Smith, A. Lanzirotti and J. Miklossy, Synchrotron-based infrared and X-ray imaging shows focalized accumulation of Cu and Zn co-localized with β-amyloid deposits in Alzheimer's disease, J. Struct. Biol., 2006, 155, 30–37.

5 S. A. James, Q. I. Churches, M. D. de Jonge, I. E. Birchall, V. Streltsov, G. McColl, P. A. Adlard and D. J. Hare, Iron, Copper, and Zinc Concentration in Aβ Plaques in the APP/PS1 Mouse Model of Alzheimer's Disease Correlates with Metal Levels in the Surrounding Neuropil, ACS Chem Neurosci, 2017, 8, 629–637.

6 J. Xu, S. J. Church, S. Patassini, P. Begley, H. J. Waldvogel, M. A. Curtis, R. L. M. Faull, R. D. Unwin and G. J. S. Cooper, Evidence for widespread, severe brain copper deficiency in Alzheimer's dementia, Metallomics, 2017, 9, 1106–1119.

7 M. Rana and A. K. Sharma, Cu and Zn interactions with Aβ peptides:consequence of coordination on aggregation and formation of neurotoxic soluble Aβ oligomers, Metallomics, 2019, 11, 64–84.

8 C. J. Sarell, S. R. Wilkinson and J. H. Viles, Substoichiometric Levels of Cu^{2+} Ions Accelerate the Kinetics of Fiber Formation and Promote Cell Toxicity of Amyloid-β from Alzheimer Disease, J. Biol. Chem., 2010, 285, , 41533–41540.

9 C. S. Atwood, R. D. Moir, X. Huang, R. C. Scarpa, N. M. E. Bacarra, D. M. Romano, M. A. Hartshorn, R. E. Tanzi and A. I. Bush, Dramatic Aggregation of Alzheimer Aβ by Cu(II) Is Induced by Conditions Representing Physiological Acidosis, J. Biol. Chem., 1998, 273, 12817–12826.

10 E. House, M. Mold, J. Collingwood, A. Baldwin, S. Goodwin and C. Exley, Copper Abolishes the β-Sheet Secondary Structure of Preformed Amyloid Fibrils of Amyloid-β_{42}, J. Alzheimers Dis., 2009, 18, 811–817.

11 J. Zou, K. Kajita and N. Sugimoto, Cu^{2+} Inhibits the Aggregation of Amyloidβ-Peptide(1-42) in vitro, Angew. Chem. Int. Ed., 2001, 40, 2274–2277.

12 J. T. Pedersen, J. Østergaard, N. Rozlosnik, B. Gammelgaard and N. H. H. Heegaard, Cu(II) Mediates Kinetically Distinct, Non-amyloidogenic Aggregation of Amyloid-β Peptides, J. Biol. Chem., 2011, 286, 26952–26963.

13 J. H. Viles, Metal ions and amyloid fiber formation in neurodegenerative diseases.Copper, Zinc and Iron in Alzheimer's, Parkinson's and Prion disease, Coord. Chem. Rev., 2012, 256, 2271–2284.

14 D. P. Smith, G. D. Ciccotosto, D. J. Tew, M. T. Fodero-Tavoletti, T. Johanssen, C. L. Masters, K. J. Barnham and R. Cappai, Concentration Dependent Cu^{2+} Induced Aggregation and Dityrosine Formation of the Alzheimer's Disease Amyloid-β Peptide, Biochemistry, 2007, 46, 2881–2891.

15 C. J. Matheou, N. D. Younan and J. H. Viles, Cu^{2+} accentuates distinct misfolding of Aβ (1–40) and Aβ (1–42) peptides, and potentiates membrane disruption, Biochem. J., 2015, 466, 233–242.

16 E. Sitkiewicz, M. Kłoniecki, J. Poznański, W. Bal and M. Dadlez, Factors Influencing Compact–Extended Structure Equilibrium in Oligomers of Aβ1–40 Peptide—An Ion Mobility Mass Spectrometry Study, J. Mol. Biol., 2014, 426, 2871–2885.

17 B. Michalke, M. Lucio, A. Berthele, B. Kanawati, Manganese speciation in paired serum and CSF samples using SEC-DRC-ICP-MS and CE-ICP-DRC-MS, Anal. Bioanal. Chem., 2013, 405, 2301-2309.

18 S. S. Aleksenko, M. Matczuk, X. Lu, L. S. Foteeva, K. Pawlak, A. R. Timerbaev, M. Jarosz, Metallomics for drug development: an integrated CE-ICP-MS and ICP-MS approach reveals the speciation changes for an investigational ruthenium(III) drug bound to holo-transferrin in simulated cancer cytosol, Metallomics, 2013, 5, 955-963.

19 T. N. S. Huynh, C. Vidaud, A. Hagège, Investigation of uranium interactions with calcium phosphate-binding proteins using ICP/MS and CE-ICP/MS, Metallomics, 2016, 8, 1185–1192.

20 K. Poléc, M. Perez-Calvo, O. Garcıa-Arribas, J. Szpunar, B. Ribas-Ozonas, R. Lobinski, Investigation of metal complexes with metallothionein in rat tissues by hyphenated techniques, J. Inorg. Biochem., 2002, 88, 197–206.

21 S. Sabella, M. Quaglia, C. Lanni, M. Racchi, S. Govoni, G. Caccialanza, A. Calligaro, V. Bellotti and E. D. Lorenzi, Capillary electrophoresis studies on the aggregation process of β-amyloid 1-42 and 1-40 peptides, Electrophoresis, 2004, 25, 3186–3194.

22 R. Colombo, A. Carotti, M. Catto, M. Racchi, C. Lanni, L. Verga, G. Caccialanza and E. De Lorenzi, CE can identify small molecules that selectively target soluble oligomers of amyloid β protein and display antifibrillogenic activity Electrophoresis, 2009, 30, 1418–1429.

23 R. A. Picou, I. Kheterpal, A. D. Wellman, M. Minnamreddy, G. Ku and S. D. Gilman, Analysis of Aβ (1-40) and Aβ (1-42) monomer and fibrils by capillary electrophoresis, J. Chromatogr. B, 2011, 879, 627–632.

24 D. Brinet, J. Kaffy, F. Oukacine, S. Glumm, S. Ongeri and M. Taverna, An improved capillary electrophoresis method for in vitro monitoring of the challenging early steps of Aβ1–42 peptide oligomerization: Application to anti-Alzheimer's drug discovery, Electrophoresis, 2014, 35, 3302–3309.

25 F. Bisceglia, A. Natalello, M. M. Serafini, R. Colombo, L. Verga, C. Lanni and E. De Lorenzi, An integrated strategy to correlate aggregation state, structure and toxicity of Aβ 1–42 oligomers, Talanta, 2018, 188, 17–26.

26 Y. Shen, S. J. Berger, G. A. Anderson and R. D. Smith, High-Efficiency Capillary Isoelectric Focusing of Peptides, Anal. Chem., 2000, 72, 2154–2159.

27 J. Chamoun and A. Hagège, Sensitivity enhancement in capillary electrophoresis-inductively coupled plasma-mass spectrometry for metal/protein interactions analysis by using large volume stacking with polarity switching, J. Anal. At. Spectrom, 2005, 20, 1030–1034.

28 S. Sauge-Merle, D. Lemaire, R. W. Evans,C. Berthomieu, J. Aupiais, Revisiting binding of plutonium to transferrin by CE-ICP-MS, Dalton Trans., 2017, 46, 1389-1396.

29 M. Deleanu, J.-F. Hernandez, L. Cipelletti, J.-P. Biron, E. Rossi, M. Taverna, H. Cottet and J. Chamieh, Unraveling the Speciation of β-Amyloid Peptides during the Aggregation Process by Taylor Dispersion Analysis, Anal. Chem., 2021, 93, 6523–6533.

30 J. E. Sonke and V. J. M. Salters, Disequilibrium effects in metal speciation by capillary electrophoresis inductively coupled plasma mass spectrometry (CE-ICP-MS); theory, simulations and experiments, The Analyst, 2004, 129, 731-738.

31 M. Mold, L. Ouro-Gnao, B. M. Wieckowski and C. Exley, Copper prevents amyloid-β1–42 from forming amyloid fibrils under near-physiological conditions in vitro, Sci. Rep., 2013, 3, 1256.

Table 1: Electrophoretic mobilities and hydrodynamic radii of the different species present in $A\beta_{1-42}$ samples

	$A\beta_{1-42}$ 100 µM in NH_4OH 0.1%				$A\beta_{1-42}$ 100 µM in Tris, pH 7.4			
CE experiments	$\mu_{ep,1}$ (x 10^8 $m^2.V^{-1}.s^{-1}$)	$\%_{species\ 1}$	$\mu_{ep,2}$ (x 10^8 $m^2.V^{-1}.s^{-1}$)	$\%_{species\ 2}$	$\mu_{ep,1}$ (x 10^8 $m^2.V^{-1}.s^{-1}$)	$\%_{species\ 1}$	$\mu_{ep,2}$ (x 10^8 $m^2.V^{-1}.s^{-1}$)	$\%_{species\ 2}$
	-0.98 ± 0.02	74 ± 4	-2.10 ± 0.05	26 ± 2	-0.94 ± 0.03	53 ± 4	-2.13 ± 0.07	47 ± 4
TDA experiments	$R_{H,1}$ (nm)	$\%_{species,1}$	$R_{H,2}$ (nm)	$\%_{species\ 2}$	$R_{H,1}$ (nm)	$\%_{species,1}$	$R_{H,2}$ (nm)	$\%_{species\ 2}$
	1.3	72 ± 7	6.6 ± 0.9	28 ± 3	1.3 ± 0.2	54 ± 6	4.2 ± 0.7	46 ± 6

Table 2: Influence of amyloid-β: Cu(II) stoichiometry on the apparent aggregation velocity

Amyloid-β: Cu(II) initial ratio	$v_{max,\ app}$ (%.s^{-1})	% monomers involved in oligomeric forms at the plateau
1: 0	$1.9x10^{-6}$	65
1: 0.1	$2.0x10^{-6}$	77
1: 0.5	$1.4x10^{-5}$	74

Table 3 : Repetability, linearity and limits of detection determined in both CE-UV and CE-ICP-MS using $A\beta_{1-16}$ and $A\beta_{1-42}$

	CE-UV	CE-ICP-MS
Migration times RSD[a]	3%	
Peak area RSD[b]	< 5 %	< 15 %
Linearity[b]	r^2 = 0.9997 (range : 5 - 100µM)	r^2 = 0.991 (range : 1.25 - 25µM)
Limit of quantification[b]	6.5 µM $A\beta_{1-16}$	0.6 µM Cu

[a] measured using $A\beta_{1-42}$

[b] measured using $A\beta_{1-16}$

Figures

Figure 1: Electrophoretic profiles of obtained by CE-UV (a,c) and taylorgrams obtained by TDA-UV (b,d).
Samples: 100 µM $A\beta_{1-42}$ at t=0 after dilution in 0.1% NH_4OH (A,B) and at t=48h after dilution in 10 mM Tris buffer containing 0.04% NH_4OH at pH 7.4 (c,d).
CE experimental conditions: HPC coated - capillary (75 µm i.d. x 64 cm), buffer: 10 mM Tris, 15 mM NaCl at pH 7.4, -20 kV with an assisted pressure of 0.1 psi, 25°C. Detection: UV at 200 nm at 54 cm from the inlet.
TDA experimental conditions: HPC coated - capillary (75 µm i.d. x 64 cm), buffer: 10 mM Tris, 15 mM NaCl at pH 7.4, mobilisation pressure: 0.7 psi, 25°C. Detection: UV at 200 nm at 54 cm from the inlet.

Figure 2: Influence of the voltage applied in CE on the $A\beta_{1-16}$ - Cu(II) dissociation
Electropherograms obtained in CE-ICP-MS for a 100 µM $A\beta_{1-16}$ and 10 µM Cu(II) sample (a) and a 100 µM $A\beta_{1-16}$ and 50 µM Cu(II) sample (c) at -20kV (in purple), -15kV(green), -10kV (red) and -7kV (blue).
Electropherograms are shifted in cps for sake of clarity.
Areas attributed to the gaussian peak (white bars), the tailing part (blue bars) and the Cu(II) released by the HNO_3 rinse at the end of the separation (dotted bars) for a 100 µM $A\beta_{1-16}$ and 10 µM Cu(II) sample (b) and a 100 µM $A\beta_{1-16}$ and 50 µM Cu(II) sample (d).

Figure 3: Monitoring in CE-UV of 100 µM of $A\beta_{1-42}$ aggregation over time in 10 mM Tris 15 mM NaCl (pH 7.4). (a) Electropherograms for different incubation times in the absence or the presence of either 10 or 50 µM of Cu(II). (b) Percentage of $A\beta_{1-42}$ involved in large oligomeric forms in the soluble fraction over incubation time in the absence (◆) or presence of 10 (■), and 50 µM (●) of Cu(II). Electropherograms are shifted in absorbance for sake of clarity.

Figure 4: Repartition of copper between the different oligomerization forms of 100 µM $A\beta_{1-42}$ over time followed by CE-ICP-MS in the presence of 10 µM (a, c) or 50 µM (b, d) of Cu(II).
(a, b) Electropherograms (shifted in ^{65}Cu signal intensity for sake of clarity, background signal is around 800 cps for all the electropherograms)
Peak 1 represents copper present in the large oligomeric forms, peak 2 represents both small oligomers and monomer Aβ / Cu(II) complexes, and peak 3 is likely to be the Cu(II) released from the monomer. (c, d) Percentages of soluble copper in small (●) and large (●) oligomeric forms of $A\beta_{1-42}$ peptide over time in the presence of 10 or 50 µM of Cu(II). Experimental conditions: HPC coated - capillary (75 µm i.d. x 64 cm), Buffer: 10 mM Tris, 15 mM NaCl at pH 7.4, -7 kV with an assisted pressure of 0.3 psi, 25°C. Detection: ICP-MS at m/z = 65 at the end of the capillary.

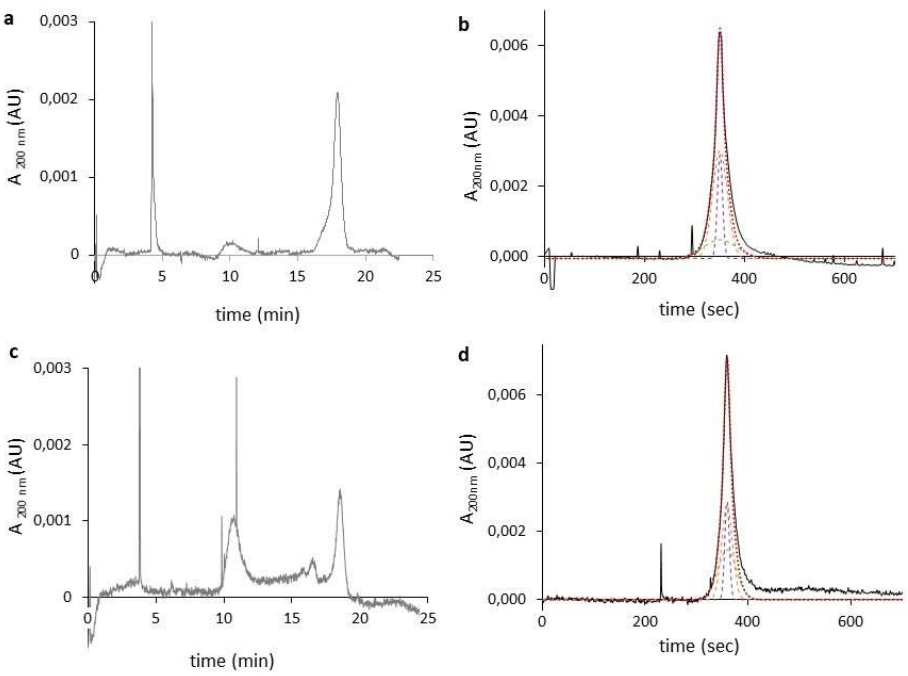
a
0,003
0,002
0,001
0
A 200 nm (AU)
0
5
10
15
20
25
time (min)
b
0,006
0,004
0,002
0,000
A200nm (AU)
0
200
400
600
time (sec)
c
0,003
0,002
0,001
0
A 200 nm (AU)
0
5
10
15
20
25
time (min)
d
0,006
0,004
0,002
0,000
A200nm (AU)
0
200
400
600
time (sec)

Figure 1

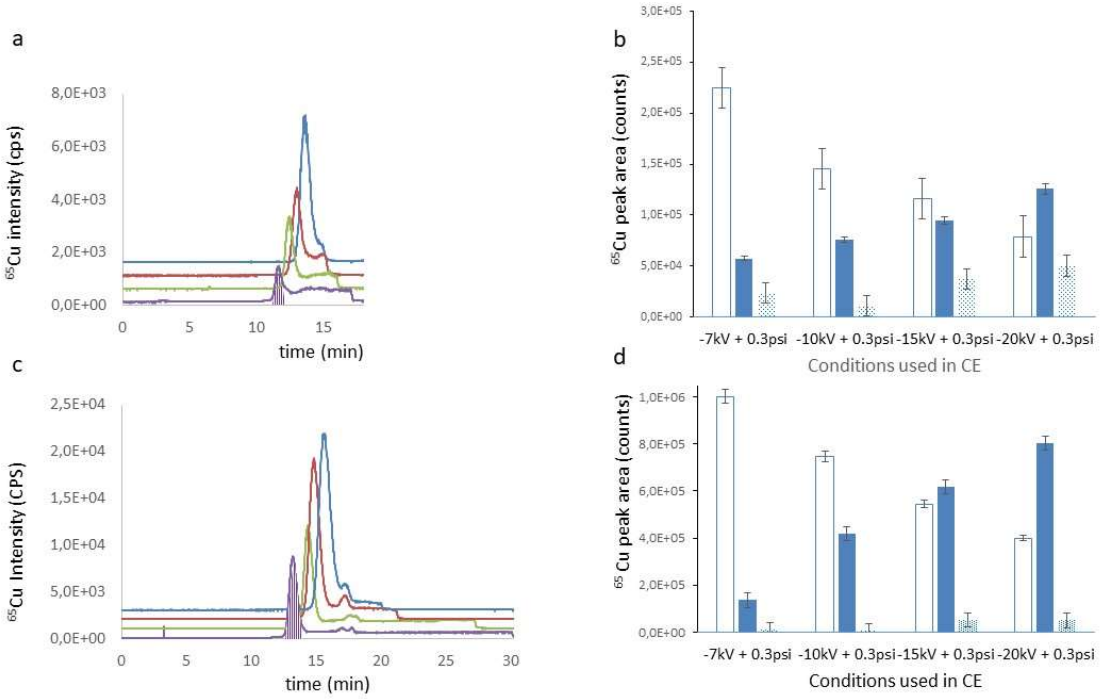
a
^{65}Cu intensity (cps)
8,0E+03
6,0E+03
4,0E+03
2,0E+03
0,0E+00
0
5
10
15
time (min)
b
^{65}Cu peak area (counts)
3,0E+05
2,5E+05
2,0E+05
1,5E+05
1,0E+05
5,0E+04
0,0E+00
-7kV + 0.3psi
-10kV + 0.3psi
-15kV + 0.3psi
-20kV + 0.3psi
Conditions used in CE
c
^{65}Cu Intensity (CPS)
2,5E+04
2,0E+04
1,5E+04
1,0E+04
5,0E+03
0,0E+00
0
5
10
15
20
25
30
time (min)
d
^{65}Cu peak area (counts)
1,0E+06
8,0E+05
6,0E+05
4,0E+05
2,0E+05
0,0E+00
-7kV + 0.3psi
-10kV + 0.3psi
-15kV + 0.3psi
-20kV + 0.3psi
Conditions used in CE

Figure 2

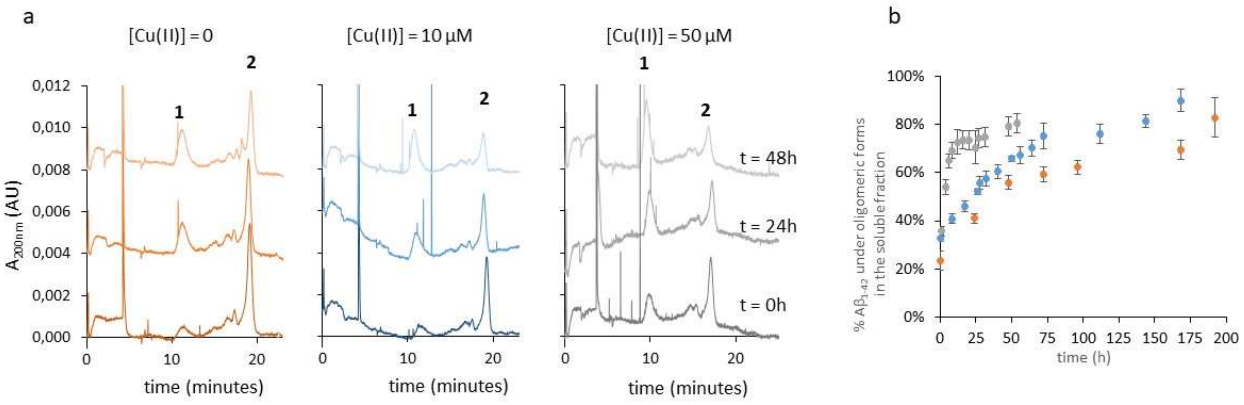
a
[Cu(II)] = 0
[Cu(II)] = 10 µM
[Cu(II)] = 50 µM
1
2
t = 48h
t = 24h
t = 0h
A200nm (AU)
time (minutes)
b
% Aβ1-42 under oligomeric forms in the soluble fraction
time (h)

Figure 3

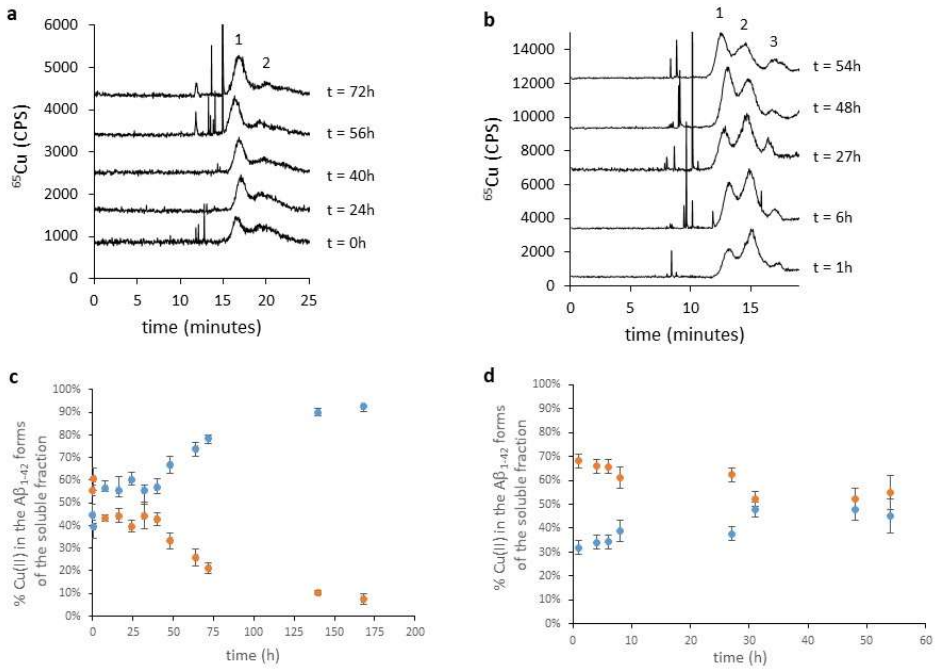
a
b
c
d
^{65}Cu (CPS)
time (minutes)
t = 72h
t = 56h
t = 40h
t = 24h
t = 0h
t = 54h
t = 48h
t = 27h
t = 6h
t = 1h
% Cu(II) in the Aβ$_{1-42}$ forms of the soluble fraction
time (h)

Figure 4